

# High-Frequency Input Impedance Characterization of Dielectric Films for Power-Ground Planes

Jan Obrzut, *Member, IEEE*, and Aleksei Anopchenko

**Abstract**—Broadband impedance characterization of high dielectric constant (high- $k$ ) films was performed using a coaxial test fixture configuration. The presented coaxial test fixture and broadband measurement methodology of impedance for high- $k$  films minimizes systematic uncertainties by reducing the interconnection inductance and improving the calibration procedure. In the APC-7 configuration, the technique enables accurate evaluation of impedance at frequencies of 100 MHz to 10 GHz with resolution of 0.01  $\Omega$ . The electrical characteristic of high- $k$  films was found to be consistent with a capacitive load without significant contribution from the circuit inductance that typically dominates the high-frequency response. The experimental data and numerical simulations showed that high- $k$  organic-ceramic composite materials could considerably suppress resonant behavior of the power-ground planes. It was found that high- $k$  organic resins filled with ferroelectric ceramic powders exhibit a high-frequency dielectric loss that increases with increasing volume fraction of the ceramic component. The dielectric dispersion and the corresponding dielectric loss of organic-ceramic hybrid materials can serve as an effective mechanism for suppressing the resonant standing waves in power-ground planes.

**Index Terms**—Decoupling capacitance, dielectric relaxation, dielectric resonators, HFSS, high- $k$  films, microwave measurements, numerical modeling.

## I. INTRODUCTION

HIGH dielectric constant (high- $k$ ) organic-ceramic hybrid materials have recently shown promise for embedded power-ground decoupling planes with desirable low impedance [1]. The power-ground planes made of typical dielectric materials exhibit undesired multiple resonance that can be mitigated by adding discrete decoupling capacitors. This approach introduces inductive components, which contribute to the equivalent inductance of the power plane and eventually limit the usable bandwidth [2], [3]. Application of thin high- $k$  dielectric layers can suppress fluctuations in impedance by damping the resonance, which extends the usable bandwidth to higher frequencies. It has been suggested that in thin layers of low loss dielectrics the resonant damping can be due to conductive losses of the metal cladding [4] and a decreased dielectric thickness [5]. In the case of organic-ceramic hybrid materials, the mechanism suppressing the resonant fluctuations of impedance is poorly understood. Evaluation of the dielectric properties of such materials requires broadband measurements, extended to the high-frequency range. However, the frequency

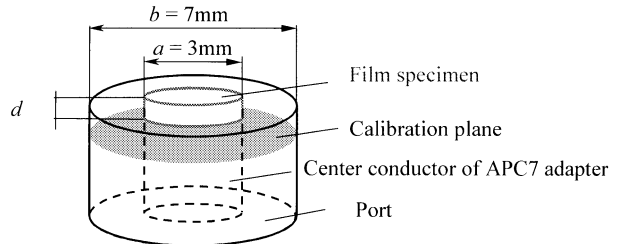


Fig. 1. Scheme of coaxial test fixture configuration.

range in which the plane shows a capacitive (dielectric) impedance characteristic is limited by the frequency of the first series resonance, which itself is influenced by the size of the specimen and inductance of the experimental set-up.

This paper describes broadband impedance measurements of high- $k$  film substrates at frequencies of 100 MHz to about 10 GHz. To extend the measurements to the microwave range, a coaxial test fixture was employed where a film specimen represents a capacitive termination. Such configuration eliminates the feeding probes and therefore, minimizes the interconnection inductance. The high-frequency dielectric relaxation mechanism in high- $k$  composite materials was analyzed using film substrates made of low loss organic resin filled with low loss ferroelectric ceramics.

## II. ANALYSIS AND MEASUREMENT PROCEDURE

The test fixture utilized an APC-7 mm precision air-filled coaxial transmission line (Fig. 1). Film specimen of thickness  $d$  and the relative complex permittivity  $\epsilon^* = \epsilon' - j\epsilon''$  was placed at the end of the center conductor of the transmission line and short terminated. The diameter of the specimen,  $a$ , matched that of the line center conductor. If  $d \ll a$ , then the primary propagation mode satisfying the boundary conditions in the specimen section is associated with the diameter of the film rather than its thickness [6]. The scattering parameter  $S_{11}$  of such network can be expressed by (1)

$$S_{11} = \frac{\rho + e^{-\gamma a}}{1 + \rho e^{-\gamma a}} \quad (1)$$

which leads to the following expression for input admittance  $Y_{in}$  of the specimen section [7]

$$Y_{in} = G_s \sqrt{\epsilon^*} \tanh \frac{\gamma a}{2}. \quad (2)$$

In (1) and (2),  $G_s$  is the characteristic conductance of the specimen,  $\rho$  is the complex reflection coefficient for nonmagnetic media;  $\rho = (1 - \sqrt{\epsilon^*}) / (1 + \sqrt{\epsilon^*})$ ,  $\gamma$  is the propagation constant,  $\gamma = j\omega/c\sqrt{\epsilon^*}$ ;  $\omega$  is the angular frequency and  $c$  is the

Manuscript received June 15, 2002; revised January 20, 2003. This work was supported in part by the NIST MSEL Director's Reserve Funds.

The authors are with the National Institute of Standards and Technology, Gaithersburg, MD 20899 USA.

Digital Object Identifier 10.1109/TIM.2003.815984

speed of light in air. Using a relation  $\tanh(jx) = j/\cot(x)$  and introducing  $x = \omega a/2c\sqrt{\epsilon^*}$  leads to expression (3), where the sample section represents a transmission line with the electrical length of  $a/2$

$$Y_{in} = G_s \frac{j\omega a}{2c} \epsilon^* \frac{1}{x \cot(x)}. \quad (3)$$

In the complex capacitance notation, the specimen capacitance,  $C_s^*$ , can be expressed as a product of the characteristic conductance per unit length and permittivity,  $C_s^* = G_s(a/2c)\epsilon^*$ . Taking into account a series residual inductance of the specimen,  $L_s$ , (3) can be rewritten as:

$$Y_{in} = \frac{j}{\frac{x \cot(x)}{\omega C_s^*} - \omega L_s}. \quad (4)$$

The inductance  $L_s$  was estimated numerically using a High Frequency Structure Simulator from Ansoft Corporation (Ansoft HFSS™) [8]. It was found that  $L_s$  is approximately proportional to the specimen thickness  $d$ , and can be compensated by an equivalent length of a loss-less transmission line. The factor,  $x \cot(x)$ , accounts for the wave propagation in the specimen section. If the electrical length,  $a$ , is small in comparison to the wavelength,  $a \ll \lambda$ ,  $x \ll 1$ , the  $L_s$  can be neglected, the value of the  $x \cot x$  approaches unity and then (4) simplifies to the input admittance of a coaxial line terminated with a shunt capacitance. The wave propagation term,  $x \cot(x)$ , has a singularity when  $x = \pi/2$ , which corresponds to the following resonance condition:

$$a = \frac{\lambda_{eff}}{2} \quad (5)$$

where  $\lambda_{eff} = \lambda/\sqrt{\epsilon^*}$  is effective wavelength. According to (5), the resonant frequency is determined by the diameter of the specimen and its complex permittivity. We employed HFSS to find numerically the three-dimensional (3-D) eigenmode solution for the specimen section and to analyze the electromagnetic field distribution in relation to the dielectric loss and the conducting losses.

The 50- $\mu\text{m}$  to 100- $\mu\text{m}$ -thick films were covered by a 50  $\mu\text{m}$  thick copper conductor on both sides. The test specimens were prepared by defining 3.0 mm diameter using photolithography. One-port measurements of the scattering parameter,  $S_{11}^m$ , were carried out using a network analyzer (Agilent 8720D). Open, short and broadband load calibration was performed using a HP 85050B APC-7 calibration kit. The relative combined standard uncertainty in geometrical capacitance measurements was 1%. The largest contributing factor to the uncertainty was the uncertainty in the film thickness measurements of 1  $\mu\text{m}$ . The relative standard uncertainty of  $S_{11}^m$  was assumed to be within the manufacturer's specification for the network analyzer. The combined relative experimental uncertainty in complex permittivity was within 8%, while the experimental resolution of the dielectric loss tangent measurements was about 0.01.

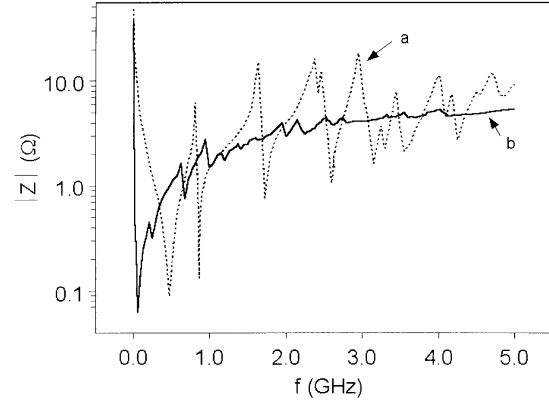


Fig. 2. Impedance of the embedded power planes. (a) 50- $\mu\text{m}$ -thick FR-4; (b) 100- $\mu\text{m}$ -thick epoxy resin loaded with PZT ceramics.

### III. RESULTS AND DISCUSSION

#### A. Impedance of Power-Ground Planes Probed in a Printed Circuit Board Test Vehicle

Fig. 2 shows results of impedance measurements for two dielectric power planes embedded in a 5 cm  $\times$  8 cm multilayer printed circuit test vehicle. Layer (a) was made of a 50- $\mu\text{m}$ -thick FR4 laminate having the dielectric constant,  $\epsilon'$ , of 3.8 at 1 GHz. Layer (b) was a 100  $\mu\text{m}$  thick high-k composite with  $\epsilon'$  of 39 at 1 GHz [9]. Both dielectric films were clad by 50  $\mu\text{m}$  thick copper. The measurements were taken at the geometrical center of the board using a G-S-G semi-rigid testing probe. The result for layer (a) shows a well known undesired resonant behavior. A series resonance at about 480 MHz is followed by a first cavity resonance at about 930 MHz. At higher frequencies, the layer (a) exhibits several resonant oscillations, due to excitation of higher order modes. Such complicated impedance characteristics may be analyzed by a cavity model with LC series branches [10], or as a network of lossy transmission lines [5]. In contrast to the layer (a), the high-k plane (layer b) exhibits the smoother characteristic. The series resonance is shifted to about 65 MHz due to higher capacitance, while the first cavity resonance is shifted to about 300 MHz due to decreased velocity of the propagating wave. The oscillation of the input impedance resulting from the first cavity resonance is considerably suppressed. Likewise, the subsequent oscillations corresponding to higher order resonant modes in layer (b) are also suppressed. Since both layers (a) and (b) have the same copper clad finish, it is evident that the observed suppression of the resonance cannot be attributed to the conductive losses in the copper cladding. Besides, the suppression cannot be ascribed to a small dielectric thickness since the layer (b) is twice as thick as the layer (a). Therefore, the dumping mechanism must arise from the dielectric properties of the high-k hybrid material, which is intriguing as such materials are typically formulated from low loss components.

In order to analyze this dumping effect in more detail broadband measurements in extended frequency range are required. Fig. 2 demonstrates that direct measurements on large power planes are not convenient for such analysis since the measured input impedance increases considerably at higher frequencies. In the case of layer (b) the impedance increases from a minimum at 65 MHz to about 5  $\Omega$  at 5 GHz resulting from uncom-

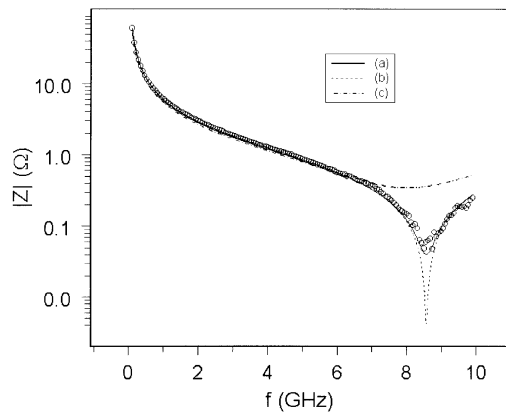


Fig. 3. Input impedance of a high-k specimen measured in coaxial configuration. Circles—experiment; lines are calculated from the inverse of (4): (a)  $\epsilon^* = 34.6 - j1.6$ , (b)  $\epsilon^* = 34.6 - j0.16$ , and (c)  $\epsilon^* = 34.6 - j16$ .

compensated inductance of the testing probe. Short-Open-Load calibration standards built into the test vehicle could have improved the impedance measurements at higher frequencies, but such approach is often unreliable. By contrast, in the coaxial test fixture configuration the inductance of testing leads is largely eliminated. This permits more accurate evaluation of impedance, especially at microwave frequencies.

#### B. Impedance Measured in Coaxial Configuration

Fig. 3 shows example impedance measurements of a model high-k composite film 80- $\mu\text{m}$ -thick having permittivity of  $34.6 - j1.6$ . This material was made to imitate the electrical properties of the power plane layer (b). The specimen consists of a low loss polymer resin (poly trimethylolpropane triacrylate) filled in 40 vol. % by a low loss barium titanate powder (TMPTA-BT) [11]. The results shown in Fig. 3 reflect the electrical characteristics of the high-k TMPTA-BT specimen, which is consistent with a capacitive load, without significant contribution from inductive components that dominate the high-frequency response (cf. Fig. 2). At about 8.2 GHz there is a dip of about  $0.05 \Omega$  in the impedance, which can be attributed to resonance absorption. The impedance results calculated from the inverse of (4) agree well with the experiment for the high-k composite. As predicted, the resonant frequency depends on the diameter of the specimen and its permittivity. The magnitude of the resonance depends on the dielectric loss. The calculated results shown in Fig. 3 illustrate that decreasing the dielectric loss,  $\epsilon''$ , from  $1.6$  ( $\tan(\delta) = 0.046$ ) to  $0.16$  ( $\tan(\delta) = 0.0046$ ) results in larger oscillation. By contrast, increasing the dielectric loss to about  $16$  ( $\tan(\delta) = 0.46$ ) may lead to substantial flattening of the impedance characteristic at the resonant frequency.

The effect of the dielectric loss and the conductivity of the metalized surfaces on the resonant behavior of the high-k specimen was analyzed numerically. Fig. 4 demonstrates the normal component of the magnitude of electric field distribution,  $E_z$ , calculated for the TMPTA-BT specimen in the coaxial test fixture at the resonant frequency. It is note worthy that the character of the field distribution at the resonance frequency does not depend on the dielectric constant. The magnitude of  $E_z$  exhibits a nonuniform structure extended along the specimen diameter

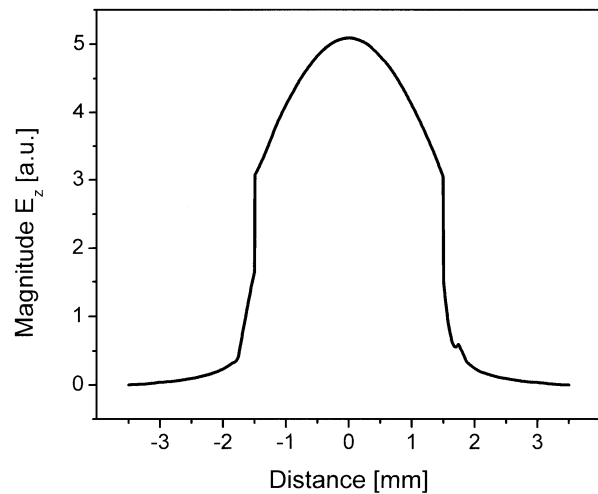


Fig. 4. Spatial distribution of the magnitude of the electric field  $E_z$  across a specimen section at the resonance frequency.

with a maximum at the center. The field appears to decay rapidly at the interface between the high-k dielectric and air. We calculated an unloaded quality factor  $Q$  for a model resonator that reassembles of the high-k specimen, which in the APC-7 configuration is surrounded by a toroidal air dielectric. Finite conductivity boundaries were assigned to all enclosed surfaces, except that part of the bottom surface is exposed to air. A perfect magnetic field ( $H$ ) was assigned to this surface with the tangential component of the  $H$ -field equal to zero. Table I lists the unloaded quality factor  $Q$  for several combinations of the dielectric loss tangent and the conductivity. It is seen that the quality factor decreases from 217 to about 2.34 when the dielectric loss tangent increases from 0.0046 to about 0.46. In comparison, analogous two order of magnitude decrease in conductivity decreases the quality factor only to about 11.7. The quality factor was found to be independent of the dielectric thickness. These results indicate that the materials dielectric loss can play a leading role in suppressing resonant behavior of the power-ground planes.

#### C. Broadband Dielectric Permittivity of High-k Organic-Ceramic Hybrid Materials

Example measurements of permittivity determined for several high-k TMPTA-BT films in relation to the volume fraction  $\varphi$  of barium titanate ( $\text{BaTiO}_3$ ) filler is shown in Fig. 5. The broadband experimental permittivity data indicate that the composites of low loss resins with low loss ferroelectric ceramics exhibit considerable dielectric dispersion. This dispersion gives rise to the frequency dependent dielectric loss. The polymer resin ( $\varphi = 0$ ) exhibits the dielectric loss maximum of only 0.11 at about 10 MHz. In comparison, the dielectric loss measured for the composites is considerably larger. According to the employed dielectric relaxation model, the frequency dependent complex permittivity can be described by four relaxation processes, three of which correspond to relaxation of the polymer matrix and one process, which corresponds to the relaxation in  $\text{BaTiO}_3$  [11]. The values of fitting parameters, where the uncertainties were estimated as 95% confidence limit in  $\chi^2$  distribution, clearly indicate that the composites exhibit multiple relaxations due to molecular dynamics of the polymer matrix.

TABLE I  
QUALITY FACTOR  $Q$  OF THE FILM SPECIMEN TREATED AS A COAXIAL CAVITY RESONATOR. THE  $Q$  VALUES WERE CALCULATED IN RELATION TO THE DIELECTRIC LOSS TANGENT  $\tan(\delta)$  AND THE CONDUCTIVITY  $\sigma$  OF THE CONDUCTOR AT THE RESONANT FREQUENCY  $f_r$

$\tan(\delta)$	$\sigma$ (S/m)	$Q$	$f_r$ (GHz)
0.0046	$5.8 \cdot 10^7$	217	10.1
0.046	$5.8 \cdot 10^7$	21.7	10.1
0.46	$5.8 \cdot 10^7$	2.3	9.4
0.0046	$5.8 \cdot 10^6$	32.2	10.0
0.0046	$5.8 \cdot 10^5$	11.7	9.7
0.0046	$5.8 \cdot 10^4$	4.2	8.8

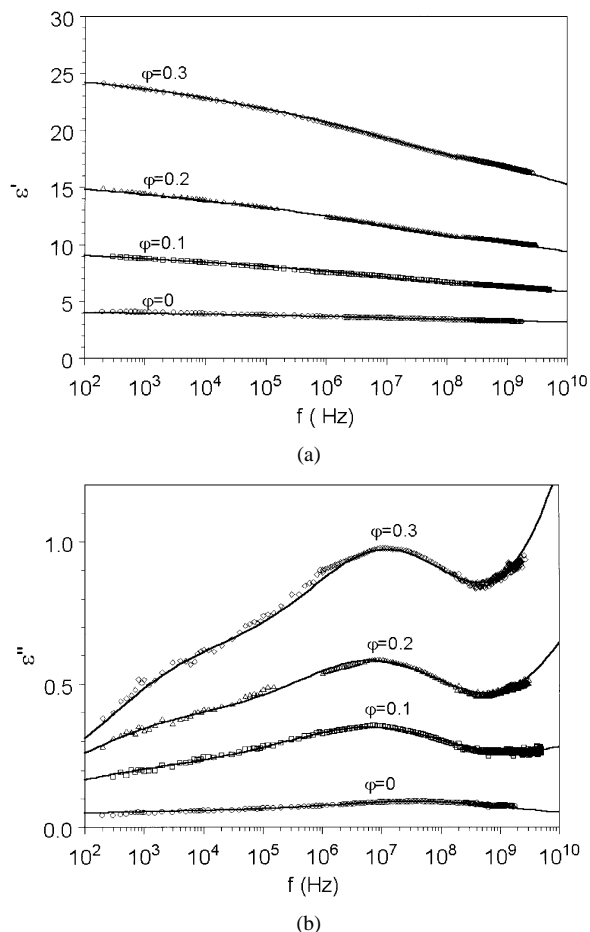


Fig. 5. (a) Dielectric constant  $\epsilon'$  of TMPTA polymer composite films for various volume fraction  $\varphi$  of barium titanate. Solid lines represent the fitting results. (b) Dielectric loss  $\epsilon''$  of TMPTA polymer composite films for various volume fraction  $\varphi$  of barium titanate. Solid lines represent the fitting results.

The dielectric increment,  $\Delta\epsilon$ , increases with increasing volume fraction,  $\varphi$ , of the ceramic component. Since the integrated loss is proportional to the dielectric increment,  $\Delta\epsilon$ , the dielectric dispersion of the polymer resin is amplified when the volume frac-

tion of the ceramics increases. Consequently, the magnitude of the dielectric loss increases with increasing content of barium titanate. In comparison, the relaxation frequency depends primarily on the dielectric properties of the organic resin. The experimental results show that the character of the dielectric loss spectra does not change with increasing fraction of  $\text{BaTiO}_3$ . The position of the loss peak is determined primarily by relaxation of the polymer matrix. Therefore, a good dielectric material for power-ground planes applications can be formulated using an organic resin that exhibits active relaxation mode at or above the clock frequency.

Considering the results of the numerical simulations and the experimental permittivity data it appears that the high-frequency loss identified in high-k organic/ceramic films can be of a significant factor in suppressing the resonant behavior of the power-ground planes as it is shown in Fig. 2(b). Such characteristic can minimize electromagnetic noise in the power bus, and thus, making the high-k composites attractive for low impedance power planes in high-speed electronic circuits.

#### IV. CONCLUSION

The presented coaxial test fixture and broadband measurement methodology of impedance for high-k films minimizes systematic uncertainties by reducing the interconnection inductance and improving the calibration procedure. In the APC-7 configuration, the technique enables accurate evaluation of impedance at frequencies of 100 MHz to 10 GHz with resolution of  $0.01 \Omega$ . The electrical characteristic of high-k films was found to be consistent with a capacitive load, without a significant contribution from the circuit inductance that typically causes a series LC resonance and dominates the high-frequency response. The experimental data and numerical simulations indicate that the materials dielectric loss can play a significant role in suppressing the resonant behavior of the power-ground planes. The suppressing effect due to the dielectric loss can be larger than that caused by the conducting losses in typical cladding. In contrast, there was no noticeable

decrease in the quality factor of model film resonators when the dielectric thickness was decreased. Organic-ceramic hybrid materials exhibit an intrinsic high-frequency relaxation process. The resulting high-frequency dielectric loss increases with the volume of the ceramic component exceeding the dielectric loss of the individual components. These dielectric characteristics of organic—ceramic composites can serve as an effective mechanism for suppressing the resonant behavior in power-ground planes.

#### ACKNOWLEDGMENT

The authors would like to thank the NCMS EDC Project, from which some of the dielectric materials and test vehicles were obtained.

**DISCLAIMER:** Certain materials and equipment identified in this manuscript are solely for specifying the experimental procedures and do not imply endorsement by NIST or that they are necessarily the best for these purposes.

#### REFERENCES

- [1] T. Hubing, "Decoupling capacitance, theory and application," in *NCMS Embedded Capacitance Conf.*, Tempe, AZ, Feb. 28–29, 2000.
- [2] I. Novak, "Accuracy considerations of power-ground plane models," *IEEE Elect. Performance Electron. Packag.*, p. 153, 1999.
- [3] G.-T. Lei, R. W. Techentin, and B. K. Gilbert, "High frequency characterization of power/plane ground structures," *IEEE Trans. Microwave Theory Tech.*, vol. 47, p. 562, 1999.
- [4] I. Novak, "Lossy power distribution networks with thin dielectric layers and/or thin conductive layers," *IEEE Trans. Adv. Packag.*, vol. 23, no. 353, 2000.
- [5] L. D. Smith, R. Anderson, and T. Roy, "Power plane SPICE models and simulated performance for materials and geometries," *IEEE Trans. Adv. Packag.*, vol. 24, p. 277, 2001.
- [6] J. Obrzut and R. Nozaki, "Broadband characterization of dielectric films for power-ground decoupling," in *IEEE IMTC*, vol. 2, 2001, p. 1000.
- [7] R. Nozaki and J. Obrzut, "Broadband complex permittivity measurements of solid films at microwave frequencies," unpublished.
- [8] J. Obrzut and A. Anopchenko, "Numerical analysis of coaxial line terminated with complex gap capacitance," *IEEE IMTC*, vol. 2, p. 1074, 2003.

- [9] Test vehicles with embedded dielectric layers a and b, obtained from NCMS, Ann Arbor, MI.
- [10] M. Xu, Y. Ji, T. H. Hubing, TP. Van Doren, and J. L. Drewniak, "Development of a closed-form expression for the input impedance of power-ground plane structures," in *Electromagn. Compatibility Int. Symp.*, vol. 1, 2000, pp. 77–82.
- [11] N. Noda and J. Obrzut, "High frequency dielectric relaxation in polymers filled with ferroelectric ceramics," in *Mater. Res. Symp. Proc.*, vol. 698, 2002, pp. EE3.8.1–EE3.8.6.

**Jan Obrzut** (M'00) received the Ph.D. degree in technical sciences from the Institute of Physics, Cracov Polytechnic, Cracov, Poland, in 1981.

After a postdoctoral appointment at the Polymer Science Department, University of Massachusetts, Amherst, he was a Researcher at the Five College Radio Astronomy Department, Amherst, working on microwave dielectric waveguides. He joined IBM in 1988 as an Advisory Engineer where he was conducting exploratory work on the application of polymer dielectrics in microelectronics. He has been with the Polymers Division, National Institute of Standards and Technology, Gaithersburg, MD, since 1997, where he performs research on the metrology of dielectric films and hybrid materials for microwave and electronic applications. His research interests include molecular dynamics and interfacial interactions in polymers, blends, and nanocomposites. Dr. Obrzut is a member of American Physical Society.

**Aleksei Anopchenko** was born in Nizhnevartovsk, Russia, in 1970. He graduated from Kharkov Polytechnic Institute, Ukraine, in 1993 and received the Ph.D. degree in solid state physics from Comenius University, Bratislava, Slovakia, in 2001.

He was an Engineer with the B. I. Verkin Institute for Low Temperature Physics and Engineering, National Academy of Sciences, from 1993 to 1997. From 1997 to 2001, he held the position of Research Associate at the Institute of Physics, Slovak Academy of Sciences. Since 2001, he has been a Guest Researcher with the Polymers Division, National Institute of Standards and Technology, Gaithersburg, MD. His current research interests include analysis of discontinuities in transmission lines, simulations of high-frequency electromagnetic field distribution in 3-D structures, application of microwave techniques for broad band permittivity measurements of polymer composites and biological substances, dielectric properties and molecular dynamics of glass formers, x-ray scattering techniques, low dimensional, and interfacial phenomena.